A high-order finite-difference linear seakeeping solver tool for calculation of added resistance in waves

Amini-Afshar, Mostafa; Bingham, Harry B.; Read, Robert

Publication date:
2015

(Abstract submitted to the 30th IWWWFB workshop, Bristol, UK, 2015)

A high-order finite-difference linear seakeeping solver tool for calculation of added resistance in waves *

Mostafa Amini Afshar, Harry B. Bingham, and Robert Read
Department of Mechanical Engineering, Technical University of Denmark
E-mail: maaf@dtu.dk, hbb@dtu.dk, rrea@mek.du.dk

1 Introduction

During recent years a computational strategy has been developed at the Technical University of Denmark for numerical simulation of water wave problems based on the high-order finite-difference method, [2],[4]. These methods exhibit a linear scaling of the computational effort as the number of grid points increases. This understanding is being applied to develop a tool for predicting the added resistance (drift force) of ships in ocean waves. We expect that the optimal scaling properties of this solver will allow us to make a convincing demonstration of convergence of the added resistance calculations based on both near-field and far-field methods. The solver has been written inside a C++ library known as **Overture** [3], which can be used to solve partial differential equations on overlapping grids based on the high-order finite-difference method. The resulting code is able to solve, in the time domain, the linearised potential flow forward-speed hydrodynamic problems; namely the steady, radiation and diffraction problems. The near-field formulation of the wave drift force has also been implemented, and development is under way to include far-field methods. This paper presents validation results based on analytical solutions for exact geometries.

2 Mathematical formulation

A moving Cartesian coordinate system *O-xyz* is adopted, which is in steady translation with the body's forward speed U. The origin of the coordinate system is at the mean free surface position, and z is vertically upward. The body is under the action of incoming waves, and is free to oscillate in 6 degrees of freedom. Assuming a potential flow model, the governing equation is:

$$\nabla^2\phi = \frac{\partial^2\phi}{\partial x^2} + \frac{\partial^2\phi}{\partial y^2} + \frac{\partial^2\phi}{\partial z^2} = 0, \quad \text{where} \quad \phi = -Ux + \phi_b + \phi_u \ \text{ and } \ \phi_u = \phi_0 + \phi_s + \sum_{k=1}^{6}\phi_k.$$

$-Ux + \phi_b$ arises due to the forward speed of the body, and represents the solution of the steady wave resistance problem. For the Neumann-Kelvin linearisation ($\phi_b = 0$), and for the double-body linearisation, the following boundary value problem is solved to obtain the base flow, $\phi_b = \phi_{db}$.

$$\nabla^2\phi_{db} = 0, \quad \frac{\partial\phi_{db}}{\partial n} = \vec{W}\cdot\mathbf{n} \ \text{ on } s_0, \quad \frac{\partial\phi_{db}}{\partial z} = 0 \ \text{ on } z = 0, \quad \nabla\phi_{db} \to 0 \ \text{ in the far field,}$$

where and $\vec{W} = (U, 0, 0)$. Moreover ϕ_0 and ϕ_s are the velocity potentials of the incident waves and the scattered waves respectively, while the body is assumed to be fixed (the diffraction problem). The velocity potentials due to oscillatory motions of the body in the kth direction (the radiation problem) are given by ϕ_k. The decomposed velocity potentials mentioned above are substituted into the non-linear boundary conditions. The linearised conditions are then obtained by Taylor-series expansion around the mean water level $z = 0$ and mean body position s_0 respectively:

$$\frac{\partial\phi_u}{\partial t} = -g\eta_u + U\frac{\partial\phi_u}{\partial x} - \nabla\phi_b\cdot\nabla\phi_u - \frac{1}{2}\nabla\phi_b\cdot\nabla\phi_b + U\frac{\partial\phi_b}{\partial x} - g\eta_b = 0, \tag{1}$$

$$\frac{\partial\eta_u}{\partial t} = \frac{\partial\phi_u}{\partial z} + U\frac{\partial\eta_u}{\partial x} - \nabla\phi_b\cdot\nabla\eta_u + \eta_u\frac{\partial^2\phi_b}{\partial z^2} - \nabla\phi_b\cdot\nabla\eta_b + U\frac{\partial\eta_b}{\partial x} + \eta_b\frac{\partial^2\phi_b}{\partial z^2} = 0. \tag{2}$$

and

$$\frac{\partial\phi_u}{\partial n} = \sum_{k=1}^{6}(\dot{\xi}_k\cdot n_k + \xi_k\cdot m_k), \quad \text{and} \quad \frac{\partial\phi_s}{\partial n} = -\nabla\phi_0(\mathbf{r},t)\cdot\mathbf{n}, \qquad \text{on } z = s_0.$$

*The authors wish to thank the Danish Maritime Fund for supporting this work.

Here, ξ_k is the translation or rotation of the body, and $\dot{\xi}_k$ is the corresponding velocity. The normal vectors n_k and the m terms are defined as follows:

$$(n_1, n_2, n_3) = \mathbf{n}, \qquad (m_1, m_2, m_3) = (\mathbf{n} \cdot \nabla)(\vec{W} - \nabla\phi_b),$$
$$(n_4, n_5, n_6) = (\mathbf{r} \times \mathbf{n}), \qquad (m_4, m_5, m_6) = (\mathbf{n} \cdot \nabla)\Big(\mathbf{r} \times (\vec{W} - \nabla\phi_b)\Big),$$

where $\mathbf{r}$ is the position vector. The above mentioned linear initial boundary value problem is solved in the time domain. Instead of finding the radiation and diffraction impulse response functions, the response of the body is calculated when exposed to a pseudo-impulsive Gaussian forcing given by $\xi_k(t) = \zeta_0(t) = e^{-2\pi^2 s^2 t^2}$, where s is a parameter to control the shape of the pseudo impulse. ζ_0 is the amplitude of the incident waves for the diffraction problem. Having solved for ϕ_u, the first-order force on the body can also be obtained from the linearised Bernoulli equation:

$$p = -\rho \left[\left(\frac{\partial}{\partial t} - \vec{W} \cdot \nabla \right) \phi_u - \vec{W} \cdot \nabla\phi_b + \nabla\phi_b \cdot \nabla\phi_u + \frac{1}{2}\nabla^2\phi_b \right]. \tag{3}$$

The frequency-domain added mass and damping coefficients a_{jk}, b_{jk}, and the wave exciting force coefficient X_j are then obtained by a Fourier transform of the time-domain data. The Froude-Krylov part of the wave excitation force is however, computed from the closed form expression in the frequency domain. Finally the body motion $\hat{\xi}_k$ in the frequency domain is found by solving the equations of motion:

$$\sum_{k=1}^{6} \hat{\xi}_k \left[-\omega^2 (M_{jk} + a_{jk}) + i\omega b_{jk} + c_{jk} \right] = A\, X_j, \qquad j = 1, 2, \ldots, 6 \tag{4}$$

where M_{jk} is the inertial mass, c_{jk} is the hydrostatic coefficient matrix, and A is the incident wave amplitude. The wave drift force is calculated in the frequency domain by considering the second-order pressure terms in the Bernoulli equation. All the terms in these expressions are obtained as described above, via Fourier transform of the corresponding pseudo-impulsive quantities [1].

3 The numerical method

The entire physical domain is descretised by overlapping structured and body-fitted grids using the **Ogen** grid generator. There are three sets of grid points including discretisation, interpolation and hole points. Each grid is mapped to a uniform Cartesian computational grid, where discretisation of the continuous derivatives takes place using fourth-order finite-difference schemes. There are two layers of ghost points generated to handle the derivatives at the boundaries. The continuity equation is descretised by a fourth-order centered scheme. A non-homogeneous Neumann boundary condition is applied at the body to satisfy the body boundary condition. The Dirichlet boundary condition is used to specify the velocity potential at the free surface. The resulting system of equations including the interpolation equations, and the right hand side vector b is constructed as $[A][\phi] = [b]$, and solved by a direct LU factorisation method. The free-surface conditions, (1) and (2) are integrated in time using the fourth-order Runge-Kutta method, and ϕ and η at the free surface are updated at each time step. As the free-surface conditions are in fact a system of hyperbolic equations, a special care is required to set the ghost points while evaluating the convective derivatives at the boundaries. In the region where $\vec{W} \cdot \mathbf{n} < 0$, extrapolation from the internal points is used to populate the ghost layers, which turns the centered scheme at the boundary into an upwind scheme. For the region where $\vec{W} \cdot \mathbf{n} > 0$, a Neumann condition is used to set the ghost points at the boundaries. The dynamic free-surface boundary condition and the known Neumann condition for ϕ on the body boundary can be used to derive a corresponding Neumann condition for η:

$$\nabla\eta \cdot \mathbf{n} \;=\; -\frac{1}{g}\left(\frac{\partial}{\partial t} (\nabla\phi \cdot \mathbf{n}) - U\, \nabla \left(\frac{\partial\phi}{\partial x} \right) \cdot \mathbf{n} \right) \tag{5}$$

where this expression corresponds to the Neumann-Kelvin linearisation. A similar relation can be obtained for the double-body flow linearisation. The above treatments are necessary for ensuring a stable numerical scheme and for preventing spurious reflections at the boundaries. Moreover in the case of grid stretching, the centered scheme is not suitable for evaluation of the convective derivatives. The unequal weighting of the neighboring points in the convective derivative on a stretched grid will always produce an effective downwinding in some areas of the free-surface, which leads to instability. Two remedies are available: either a centered scheme is used and at the same time a Savitzky-Golay type filter is applied to the solution at each time step, or an upwind-biased scheme is used for evaluation of the convective derivatives.

4 Results

The radiation problem for surge and heave body motion has been solved for a floating cylinder with $Fr = U/\sqrt{ga} = 0.03$, where a is radius of the cylinder. The radiation problem for sway and heave motion has been solved for a submerged sphere with $Fr = 0.40$ with a submergence depth of $h = 2a$. The diffraction problem in the case of the head waves for the submerged hemisphere with $Fr = 0.40$ has also been solved. Just the imaginary part of the complex force is shown here, and $\nu = \omega_e^2/g, \nu_0 = \omega/g$. The numerical results show very good agreement with the analytical solutions from [5] and [6]. The deep-water limit has also been shown in the figure, as the analytical results are for the deep water condition. The wave drift force along the x coordinate and the body motions have been calculated for the case of a floating hemisphere with $Fr = 0$, and results have been compared with those calculated using **WAMIT**. Contributions from both the water line integral and the body surface integral in the near-field method are shown in the figure, and d is the diameter of the hemisphere. The horizontal line in the drift force figure shows the analytical asymptotic value $-\frac{1}{3}$ for the short waves. The results of the developed solver in the figure are shown with the name *OceanWave3D*.

5 Conclusions

A seakeeping solver has been developed based on the high-order finite-difference method applied on overlapping grids. A stable numerical scheme has been achieved either by using a centered scheme and applying a mild filter to the solution, or by using the upwind-biased difference scheme for the convective derivatives in the free-surface boundary conditions. The solver has been validated for exact geometries, and work is under way to validate the code for real ship geometries. The solver is being developed to include more models for the wave drift force calculation, and to run in parallel in order to demonstrate convergence of the added resistance based on both far-field and near-field methods.

References

[1] Amini Afshar, M. *Towards Predicting the Added Resistance of Slow Ships in Waves*. PhD thesis, DTU Mechanical Engineering, 2015.

[2] Bingham, H. B. and H. Zhang. On the accuracy of finite-difference solutions for nonlinear water waves. *Journal of Engineering Mathematics*, 58(1-4):211–228, 2007.

[3] Brown, D. L., W. D. Henshaw, and D. J. Quinlan. Overture: An object-oriented framework for solving partial differential equations on overlapping grids. *Object Oriented Methods for Interoperable Scientific and Engineering Computing, SIAM*, pages 245–255, 1999.

[4] Engsig-Karup, A. P., H. B. Bingham, and O. Lindberg. An efficient flexible-order model for 3d nonlinear water waves. *Journal of computational physics*, 228(6):2100–2118, 2009.

[5] Wu, G. and R. E. Taylor. Radiation and diffraction of water waves by a submerged sphere at forward speed. *Proceedings of the Royal Society of London. A. Mathematical and Physical Sciences*, 417(1853):433–461, 1988.

[6] Wu, G. and R. E. Taylor. The hydrodynamic force on an oscillating ship with low forward speed. *Journal of Fluid Mechanics*, 211:333–353, 1990.

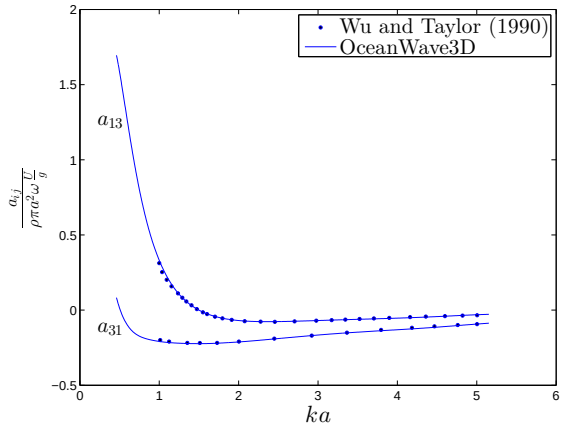

Floating cylinder, a_{13} and a_{31}

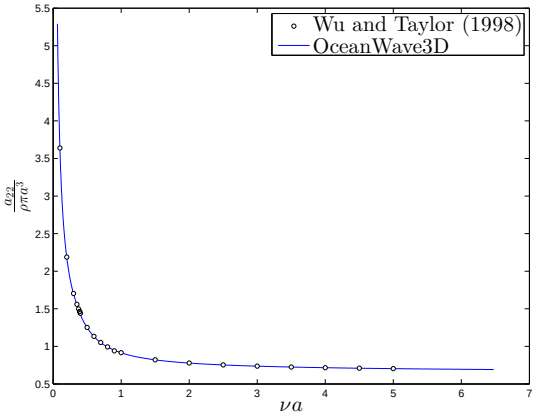

Submerged sphere, a_{22}

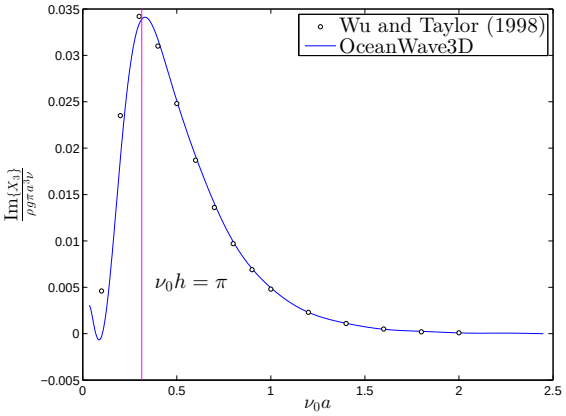

Submerged sphere, heave force imaginary

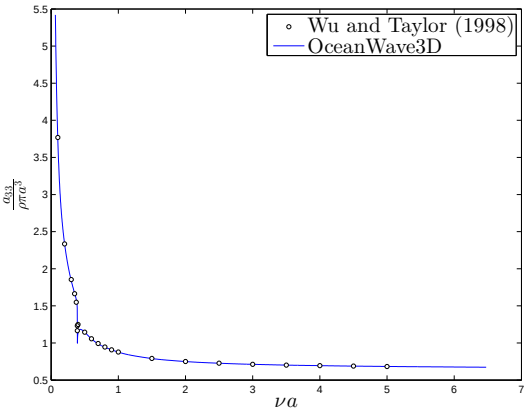

Submerged sphere, a_{33}

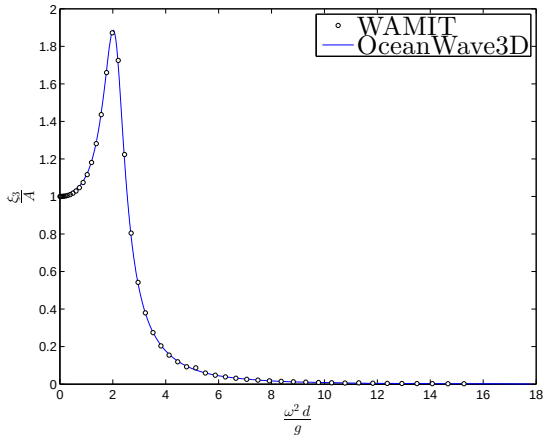

Floating hemisphere, RAO

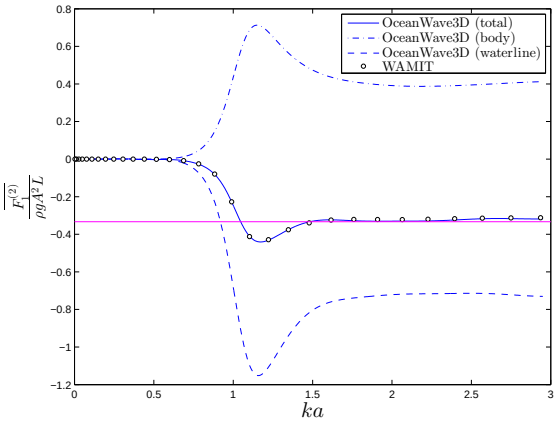

Floating hemisphere, wave drift force

Figure 1: Validation results for various quantities using a floating two-dimensional cylinder, a sumberged sphere, and a floating hemispere.